MDPI

Article

An Overview of Synthesis and Structural Regulation of Magnetic Nanomaterials Prepared by Chemical Coprecipitation

Zelin Li [1,2,†], Yuanjun Sun [3,†], Songwei Ge [1,2], Fei Zhu [1,2], Fei Yin [1,2], Lina Gu [1,2], Fan Yang [1,2,*], Ping Hu [1,2,*], Guoju Chen [3], Kuaishe Wang [1,2] and Alex A. Volinsky [4]

[1] School of Metallurgy Engineering, Xi'an University of Architecture and Technology, Xi'an 710055, China
[2] National and Local Joint Engineering Research Center for Functional Materials Processing, Xi'an University of Architecture and Technology, Xi'an 710055, China
[3] State Key Laboratory of Comprehensive Utilization of Nickel and Cobalt Resources, Jinchang 737100, China
[4] Department of Mechanical Engineering, University of South Florida, Tampa, FL 33620, USA
* Correspondence: yangfan1990@xauat.edu.cn (F.Y.); huping1985@xauat.edu.cn (P.H.)
† These authors contributed equally to this work.

Abstract: Magnetic nanomaterials are widely used in biosynthesis, catalysis, as electronic and microwave-absorbing materials, and in environmental treatment because of their high specific surface area, strong magnetism, chemical stability, and good biocompatibility. The chemical coprecipitation method is widely used for the preparation of magnetic nanomaterials due to its simplicity, low cost, and easily-controlled operating conditions. The magnetic nanomaterials prepared by the chemical coprecipitation method are summarized according to the different compositions, including the basic preparation principles, and the factors affecting their morphology, size, and microstructure. The mechanisms of preparing magnetic nanomaterials by chemical precipitation and the process control factors are emphasized. Finally, the preparation of magnetic nanomaterials by chemical coprecipitation is summarized and prospected.

check for updates

1. Introduction

In recent years, magnetic nanomaterials have been widely used in production, including ultra-microsensors, catalysts, anti-cancer medicine, biological engineering, the electronics industry, and other fields. Therefore, the preparation and applications of magnetic nanomaterials are important research topics [1–5]. Magnetic nanomaterials have applications in various fields due to their large specific surface area, extremely small size, high magnetism, and other characteristics. For example, $CoFe_2O_4$ magnetic nanomaterials as sensors have wide functions, high sensitivity, and fast response, while nanoparticles have the advantages of miniaturization and high speed [6]. Fe_3O_4 nanopowder and nano nickel, cobalt, and nickel-cobalt alloy materials are widely used as catalysts in wastewater treatment, CO catalytic oxidation, etc. [7–9]. Fe_3O_4 particles with a size smaller than 10 nm can swim in blood vessels. Therefore, magnetic Fe_3O_4 nanoparticles are used to dredge cerebral thrombosis, clean up fat accumulation in cardiac arteries, and even kill cancer cells to fight cancer. Iron oxide nanoparticles are one of the most widely used magnetic nanomaterials in the biomedical field [3,10]. Nanomaterials are used in the electronics industry to make micro-computer components [11].

There are many preparation methods for magnetic nanomaterials, such as coprecipitation, hydrothermal, sol-gel, atomization, carbonyl methods, and so on. However, the sol-gel method has some disadvantages, such as expensive raw materials, poor sintering between particles, high shrinkage during drying, and easy agglomeration. The low-temperature hydrothermal method is generally used to prepare oxide powder, and the medium of

the hydrothermal method has some limitations, including high-temperature hydrothermal process equipment requirements, technical difficulties, and poor safety performance. The carbonyl method also has high environmental requirements and is used less [12–14]. Chemical coprecipitation has become one of the common methods for preparing magnetic nanomaterials. The chemical coprecipitation method can not only make fine and uniformly mixed raw materials but also has the advantages of low preparation cost and simple preparation. The product also has good performance. The general process is as follows: select precipitant according to the substances to be precipitated → precipitate reactions → filtrate → wash → dry → obtain precipitates [15]. A flowchart of this process is shown in Figure 1. The chemical coprecipitation process is simple and suitable for large-scale industrial applications and the preparation of various nanomaterials. The main mechanisms of the preparation process are as follows [16,17].
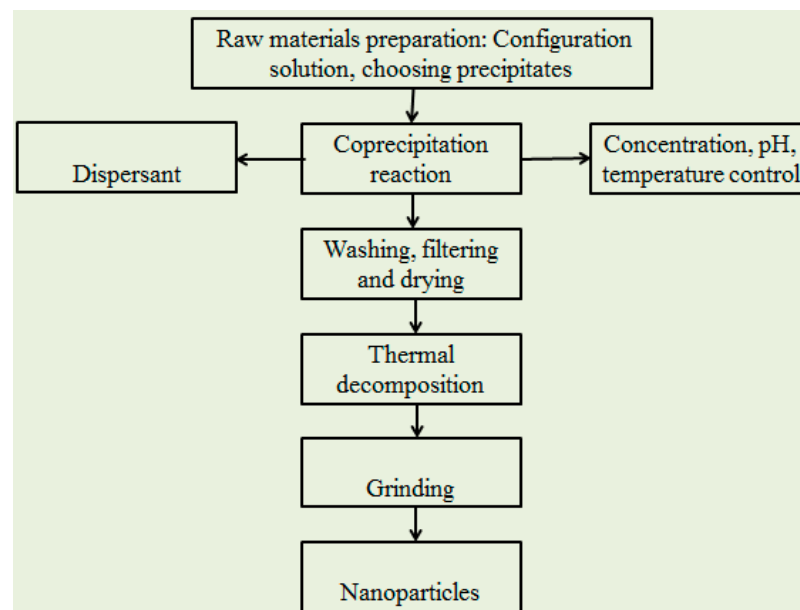

Figure 1. Flow chart of preparation of nanometer powder by chemical precipitation method.

It is well known that the premise of new phase formation is the existence of metastable states, such as supersaturation, supercooling, or overheating states. Therefore, a large supersaturation can be achieved at the usual reaction concentration. Coprecipitation reaction is the precipitation of solids from the liquid phase. Figure 2a shows a diagram of the solution supersaturation with time. As seen in Figure 2a, precipitation can only be achieved with a certain supersaturation of the solution. Based on Figure 2b, one can draw the following conclusion: the higher the supersaturation, the easier the precipitates form [16–18].

For certain supersaturation conditions, the solute molecules generated by the reaction will form new crystal nuclei during nucleation and growth. Conversely, the generated solute molecules will diffuse to the surface of the generated nuclei, and then arrange on the surface of the crystal nuclei according to the specific crystal structure to complete the crystal growth. Due to constant supersaturation, the crystal growth rate is the key to controlling molecular diffusion or molecular entry into the lattice on the crystal plane. The former is directly proportional to the supersaturation ratio, and the latter is related to the crystal interface structure. For the crystal particle growth process of oxide precursors obtained by the precipitation method, the crystal nuclei surface conforms to the rough and fine abrupt interface growth model due to low solubility and high supersaturation [17,18].
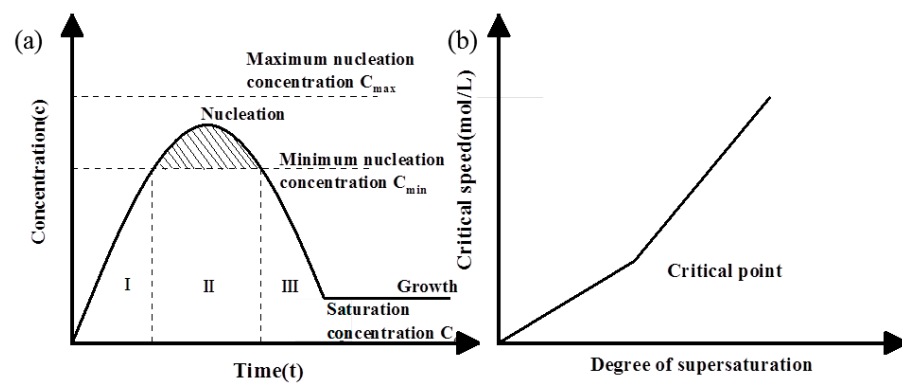
Figure 2. (**a**) Variation of supersaturation of precipitation solution with time; (**b**) relationship between nucleation rate and supersaturation [18]. (**a**,**b**) Reprinted from Central South University, open access, Copyright (2022).

In summary, it can be seen that the conditions for preparing nanomaterials by the chemical coprecipitation method are controllable and can usually be prepared in one step, which is very important for the application of the chemical coprecipitation method. Magnetic nanomaterials also play important roles in aerospace, military, magnetic materials, the battery industry, etc. To prepare magnetic nanomaterials using chemical coprecipitation, it is important to know which factors will affect the morphology, structure, size, and related properties of magnetic nanomaterials. These are the key references for the preparation of magnetic nanomaterials [19,20].

In this paper, the magnetic nanobiomaterials and magnetic nanocatalysts, magnetic nano wave-absorbing materials, nanoelectromagnetic materials, and magnetic nanoadsorbents prepared by the chemical coprecipitation method are summarized, and the effects of different conditions on the magnetic nanomaterials are discussed. This will promote the application of the chemical coprecipitation method and have profound significance for the in-depth understanding of magnetic nanomaterials.

2. Magnetic Nanobiomaterials

Magnetic nanomaterials have good application prospects as biomaterials due to their small size, good biodegradability, biocompatibility, and stability. As biomaterials, magnetic nanomaterials are mainly used in the fields of magnetically targeted drugs, immobilized enzymes, cell separation, immunoassays, and gene therapy. Due to the exchange coupling and bias effects of magnetic nanobiomaterials, they have been widely used in magnetic resonance imaging, magnetic hyperthermia, and biosensors [21,22].

Magnetic Fe_3O_4 nanomaterials have been used in clinical medicine. The magnetic Fe_3O_4 nanomaterials prepared by the chemical coprecipitation method have been studied by many researchers. The specific action process is described as follows. The raw material for preparing Fe_3O_4 nanopowder by chemical precipitation is soluble iron salt, which contains Fe^{2+} and Fe^{3+}. Generally, ammonia water is used to adjust the pH value. At a certain temperature, a coprecipitation reaction occurs under intense magnetic stirring. After the reaction proceeds for a period of time, precipitation occurs, and then the products are filtered, washed, and dried, finally obtaining Fe_3O_4 nanopowder [5]. The general reaction is [2,6]

$$8OH^- + Fe^{2+} + 2Fe^{3+} = Fe_3O_4\downarrow + 4H_2O \tag{1}$$
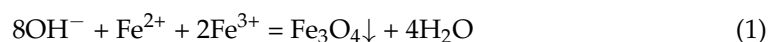
There are many factors affecting the morphology, structure, and magnetic properties of magnetic nano Fe_3O_4. Chen et al. [23] studied the effects of reaction temperature, $n(Fe^{2+})/n(Fe^{3+})$, and pH on the magnetic properties of Fe_3O_4 nanopowder. The pH has a great influence on magnetic properties. With the increase in pH, the saturation magnetization intensity (M_S) also increases. The effect of the reaction temperature on magnetic properties is non-linear. When the temperature increases from 30 °C to 40 °C, the saturation

magnetization increases, but when the temperature increases from 40 °C to 60 °C, the saturation magnetization decreases, which indicates that this is a small-scale increase, and other factors lead to the decrease of saturation magnetization. The theoretical ratio of $n(Fe^{2+})/n(Fe^{3+})$ is 1:2, but the experimental results show that it is 1:1.25. Zhang et al. [24] studied the effects of the ammonia addition on the dispersion, yield, and morphology of Fe_3O_4 nanoparticles. The results show that the prepared Fe_3O_4 nanoparticles were indeed coated with oleic acid and had good dispersion in n-octane, toluene, cyclohexane, n-hexane, and absolute ethanol organic solvents. There are two ways of adding ammonia water: dropping and direct adding. When dropping ammonia water, the Fe_3O_4 nanomaterials form as sheets with a small number of rods. When ammonia is directly added, the generated Fe_3O_4 nanomaterial is rod-shaped, which is affected by crystal dynamics, especially the free energy on the crystal surface. When the method of adding ammonia is changed from dropping to direct addition, the yield rate is greatly improved from 33% to 83%. Hu et al. [25] prepared Fe_3O_4 nanoparticles through the chemical precipitation method. The effects of stirring speeds of 320 rpm, 640 rpm, and 1400 rpm on the morphology and size of the materials were studied. Based on the X-ray diffraction results, the obtained Fe_3O_4 nanoparticles were single crystals. Transmission electron and scanning electron microscopy showed that the particle sizes of Fe_3O_4 nanoparticles increased with the stirring speed due to agglomeration. When Fe_3O_4 nanoparticles prepared at a speed of 640 revolutions per minute were applied to magnetic particle testing of samples with known crack defects, the crack defects were clearly visible, indicating that they could be used for non-destructive testing.

Many studies on the preparation of Fe_3O_4 nanomaterials were carried out without alternating or static magnetic fields applied. Li et al. [26] studied the preparation of Fe_3O_4 nanoclusters by chemical precipitation under an alternating magnetic field. The differences between the Fe_3O_4 nanoclusters prepared by alternating magnetic field-assisted coprecipitation and the Fe_3O_4 nanoclusters prepared by classical coprecipitation were compared. Through transmission electron microscopy and X-ray diffraction analysis, the morphology and structure of Fe_3O_4 nanoclusters prepared by the two methods were the same. The saturation magnetization M_S of Fe_3O_4 nanoclusters is 69.2 emu/g, the coercive force is 6 Oe, and the remanence is 0.3 emu/g. The saturation magnetization of Fe_3O_4 nanoclusters generated by the classical coprecipitation reaction is 61.3 emu/g, the coercive force is 2 Oe, and the remanence is 0.1 emu/g. Through the analysis of the infrared images, the Fe_3O_4 nanoclusters prepared by AC magnetic field-assisted coprecipitation have high heat, good biocompatibility, and high calorific value.

Ferritic compounds with the general formula MFe_xO_y—where M can be Mn, Co, Mg, Ni, Ce, Gd, and other elements—are good biomedical materials for medical and biological engineering, which can be used for immobilizing enzymes, cell separation, gene therapy, etc. Zhao et al. [27] prepared magnetic Fe_3O_4 nanomaterials through various methods, including chemical coprecipitation. The results show that Fe_3O_4 magnetic nanomaterials have good crystallinity, high stability, low toxicity, and good biological properties. Fe_3O_4 nanomaterials have a binding affinity with doxorubicin hydrochloride, an anticancer drug, and have good adaptability to the pH environment. Therefore, it is a good magnetic targeting drug medium. Ignatovich et al. [28] proved that nanomagnetic Fe_3O_4 material exhibits superparamagnetism and can combine with human proteins. Kea et al. [29] prepared $NiFe_2O_4$ nanoparticles (NPs) by coprecipitation with subsequent thermal annealing. The toxicity and biocompatibility of $NiFe_2O_4$ nanoparticles were evaluated in different cancer cell lines, and the presented physical and biological results indicated low toxicity and biocompatibility of nanoparticles. Consequently, $NiFe_2O_4$ nanoparticles can be used in targeted drug delivery, as magnetic nanoparticles for hyperthermia, magnetic resonance imaging, or cell isolation.

Figure 3a shows the general experimental procedure for the preparation of Fe_3O_4 by chemical precipitation. Figure 3b shows the preparation of gold nanoparticles containing a methotrexate (MTX) anticancer agent through a stratified double hydroxide coprecipitation-

electrostatic interaction strategy. The particles obtained have strong magnetization, high drug loading, and enhanced therapeutic effect, thus they can be used in magneto-chemical photothermal therapy. The release of the magnetic drug depends on the magnetically controlled release. Figure 3c demonstrates the process of synthesis and magnetic drug targeting of Carboxymethyl Assam Bora rice starch-coated superparamagnetic iron oxide nanoparticles (CM-ABRS SPIONS). Figure 3d shows that Fe_3O_4@PSC (PSC is short for Polydextrose sorbitol carboxyl) nanoparticles prepared by the AC electromagnetic field-assisted coprecipitation method have better thermal properties than Fe_3O_4 nanoparticles prepared by heating coprecipitation in an alternating-current magnetic field. Because of the magnetic effect induced by the alternating-current magnetic field, Fe_3O_4 nanoparticles tend to grow along the magnetization direction. Therefore, these clusters exhibit higher saturation magnetization, specific absorption, and thermal properties, which make high-performance magnetic nanomaterials promising for wider applications. In summary, magnetic nanoparticles prepared by the chemical coprecipitation method have promising applications in biomedicine [26–33].
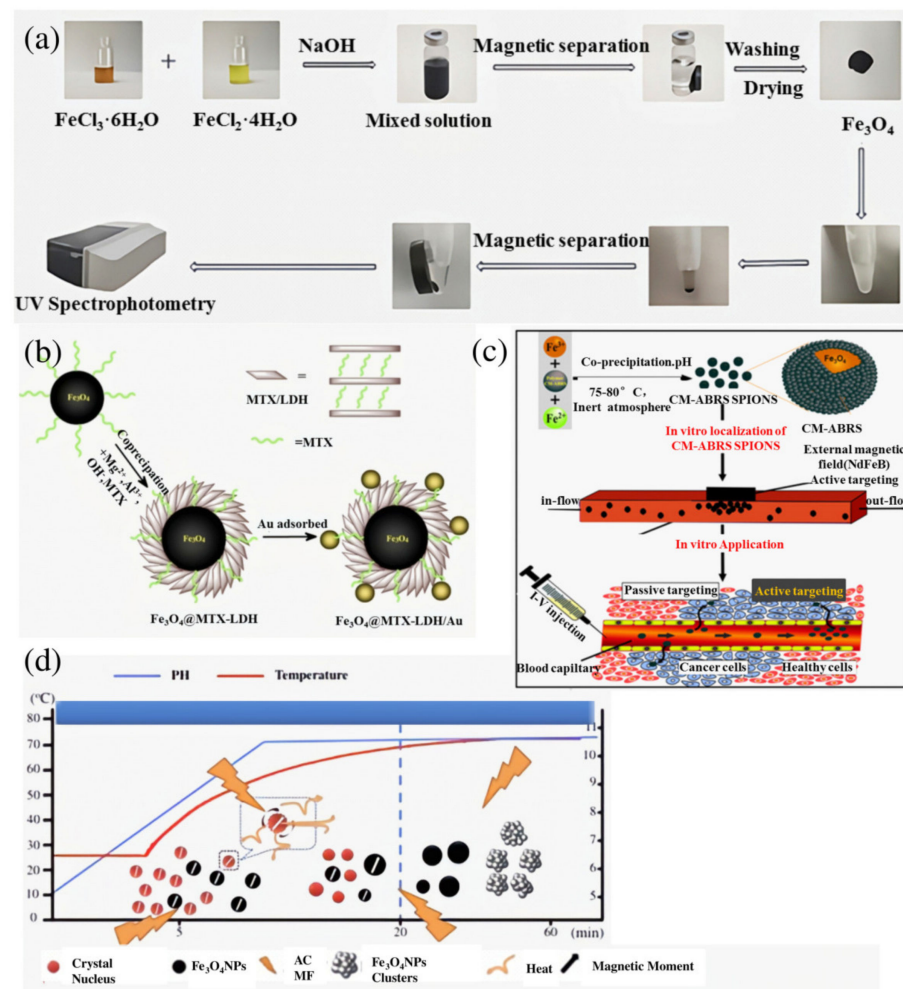
Figure 3. (**a**) Synthesis and (**b–d**) action diagrams of biomaterials [5,28–31]. (**a**) Reprinted from Chemical Engineering Journal C, 5416340606254, [30], Copyright (2022), with permission from Elsevier. (**b**) Reprinted from Materials Science & Engineering C, 5416251011560, [3], Copyright (2022), with permission from Elsevier. (**c**) Reprinted from International Journal of biomacromolecules, 1282828, [32], Copyright (2022), with permission from International Journal of biomacromolecules. (**d**) Reprinted from Colloids and Surfaces A: Physicochem. Eng. Aspects, 5416260383435, [26], Copyright (2022), with permission from Elsevier.

In summary, magnetic Fe_3O_4 nanomaterials are the most studied biomaterials at this stage. The system description is relatively complete. There are many studies on the influencing factors of magnetic Fe_3O_4 nanomaterials from preparation to the specific effects of reaction temperature, Fe^{2+}/Fe^{3+} ratio, pH, ammonia addition method, amount, and stirring speed on the magnetic properties, yield, dispersion, morphology, and size of magnetic Fe_3O_4 nanomaterials. Magnetic Fe_3O_4 nanomaterials are widely used as medical biomaterials. Generally, they are used as medical carriers to solidify biological enzymes and bind biological proteins. They can also be used as carriers of anticancer drugs to deliver the combined treatment of chemotherapy and magnetic hyperthermia in alternating magnetic fields, which is of great significance in medicine [30–33].

3. Magnetic Nanocatalysts

Magnetic nanocatalysts have a large surface area, high surface energy, and are photocatalytic. In particular, it has been found that the preparation of nanoparticles from common magnetic materials such as Fe, Ni, Co, and metal alloys can greatly improve their catalytic performance, thus nanometal alloy catalysts have good application prospects. Specifically, in recent years, researchers have made great efforts in the development of clean energy, focusing on the hydrogen evolution of electrolytic water and the reaction of CO_2 to generate methane. However, the reaction rate of these two reactions is slow under normal conditions. Therefore, finding appropriate catalysts for hydrogen evolution and methane reorganization is very important [34–41].

A good catalyst needs to have adequate basic properties such as high stability, wide pH adaptation range, and high catalytic activity. The chemical coprecipitation method can control these properties when preparing magnetic nanocatalysts. The carbon $NiFe_2O_4/Fe_2O_3$ magnetic catalyst prepared by Zheng et al. [42] is suitable for the 3–9 pH range. Under the following conditions (0.6 g $NiFe_2O_4/Fe_2O_3$, pH = 3), the degradation rate of Rhodamine (RHB) is estimated to reach 90% within 60 min. The stability of the catalyst was evaluated. The results show that it is suitable for alkaline and acidic environments and can highly degrade dyes with good stability. Cui et al. [43] studied the effects of different preparation methods (impregnation roasting, colloidal deposition, and coprecipitation on the catalytic oxidation of formaldehyde) on the activity of a Pt/Fe_3O_4 magnetic catalyst. The results showed that the Pt/Fe_3O_4 catalyst prepared by coprecipitation has good catalytic activity.

Different structures have a great influence on the catalytic activity of the catalyst. Banić et al. [44] prepared a new magnetic catalyst WO_3/Fe_3O_4 using the chemical coprecipitation method. The results show that WO_3/Fe_3O_4 has a mesoporous structure and is accompanied by the effects of semiconductor coupling, which also greatly affects the catalytic effect. Zheng et al. [45] prepared a Pt_2FeNi alloy nanocatalyst loaded with dodecyl sulfate (DS-)-intercalated NiFe layered double hydroxides (DS-NiFe LDH) through one-step hydrothermal coprecipitation, and studied the self-stripping and assembly of Pt_2FeNi alloy and DS-NiFe-LDH, which have strong bonding strength. By studying the catalytic performance of DS-NiFe-LDH and DS-NiFe-LDH-xPt, it can be seen that DS-NiFe-LDH-xPt has better catalytic activity. The interface between DS-NiFe-LDH and Pt_2FeNi is an important factor affecting the catalytic process. The catalytic performance of the DS-NiFe-LDH-xPt is caused by the increased oxidation of Pt_2FeNi. Excessive oxidation will reduce the catalytic performance of the Pt_2FeNi alloy. The fundamental reason is that the combination of Pt_2FeNi and DS-NiFe-LDH changes the chemical environment of metal atoms on the alloy surface, thus changing the catalytic performance of the alloy. The results show that DS-NiFe-LDH-xPt has good stability, durability, and catalytic activity.

In order to improve the catalytic activity of magnetic nanocatalysts, one can start with the catalyst structure. Changing the catalyst structure will also change the catalyst activity. Wu et al. [46] prepared ultra-thin $NiCo/NiCo_x$-SiO_2 nanobelts with an assembled flower cluster heterostructure using the coordination coprecipitation method. SiO_2 is stable and the 2D structure is suitable for loading a large number of active sites, thus $NiCo/NiCo_x$-SiO_2 has stable catalytic performance. During the catalytic process, it is found that the key

catalytic elements are Ni and Co, which may be due to the rich active lattice oxygen atoms in $NiCo/NiCo_x-SiO_2$ after the reduction atmosphere treatment, which can effectively improve the catalytic oxidation activity. The $NiCo/NiCo_x-SiO_2$ nanobelts have high stability and catalytic activity. Sabit et al. [47] used CdZnS and Co doping to improve the photocatalytic degradation of methylene blue by CdZnS nanoparticles. The degradation rate always increased with the increase of Co content from 0% to 5%. However, when it exceeded 5%, such as at 10%, although the Co content increased, the degradation rate did not increase but rather decreased. Therefore, the photocatalytic degradation effect of CdZnS-1 nanoparticles doped with 5% Co content in this experiment was the best doping strategy. The possible reason for this result is that the excessive Co metal in the medium enters the lattice of CdZnS-1 nanomaterial and deactivates the active region. It can be seen that Co doping CdZnS nanomaterials can significantly improve catalytic activity.

Wang et al. [48] used the chemical coprecipitation method to prepare $CuBi_2O_4$-graded microtubules and AuAg alloy-modified $CuBi_2O_4$-graded microtubules. In order to evaluate the photocatalytic performance of $CuBi_2O_4$ nanomaterials, they analyzed it by degrading the RHB solution. The $CuBi_2O_4$ nanomaterial modified by AuAg further enhances its photocatalysis. The prepared $AuAg-CuBi_2O_4$ nanomaterial shows that $CuBi_2O_4$ microtubules are transferred to the surface of AuAg nanoparticles, indicating that there are more photoelectron and hole transfers, which can participate in the photocatalytic reaction. Photoelectron and hole transfers are further studied by photocurrent response and electrochemical impedance spectroscopy (EIS). It is found that the rate of photogenerated electrons and holes in $AuAg-CuBi_2O_4$ nanotubes is faster, which proves that the catalytic activity of $AuAg-CuBi_2O_4$ nanotubes is better. The stability of the $AuAg-CuBi_2O_4$ nanotube photocatalyst also shows good stability.

Figure 4a shows the catalytic performance of the modified $BaFe_{12}O_{19}$ prepared by the coprecipitation method, which is greatly improved after being modified by WC. The phenomenon indicates that the modified magnetic catalyst can be used to improve the catalytic performance of the magnetic catalyst. Figure 4b is a schematic diagram of the process for preparing porous Ni-Co alloy electrodes using a dynamic hydrogen bubble template of electrodeposition technology and a schematic diagram of the catalytic total hydrolysis of water by porous Ni-Co alloy electrodes. The invention provides catalytic sites. Therefore, the catalytic activity of the Ni-Co alloy was increased. Figure 4c shows the effects of magnetic nanocatalysts on the degradation of dyes in wastewater, which can be seen clearly, illustrating the prospect of magnetic nanocatalysts for wastewater treatment. As the main magnetic catalyst, the structure of the nano-Ni-Co catalyst is seldom expressed, so the crystal structure of $NiCo_2O_4$ in Figure 4d can be used as a reference structure [47–60].

In the aforementioned research, magnetic nanocatalysts involve a variety of elements and a wide range of materials. A large number of scholars have studied the preparation of nanocatalysts and influencing factors such as morphology, size, structure, and catalytic activity during the preparation process. The research shows that different morphology and structure have a great impact on the activity of various nanomaterials, and the means to improve the activity of nanocatalysts are limited, so it is necessary to change the chemical environment of active particles. Loading 2D nanomaterials or doping nanoparticles is an effective way to improve the activity of catalysts, and preparing them into mesoporous materials is another way. Table 1 compares the catalytic performance of some nano-Ni-Co alloy powders as catalysts. It can be seen that the catalysts with special structures and doping have good catalytic performance [54–60].
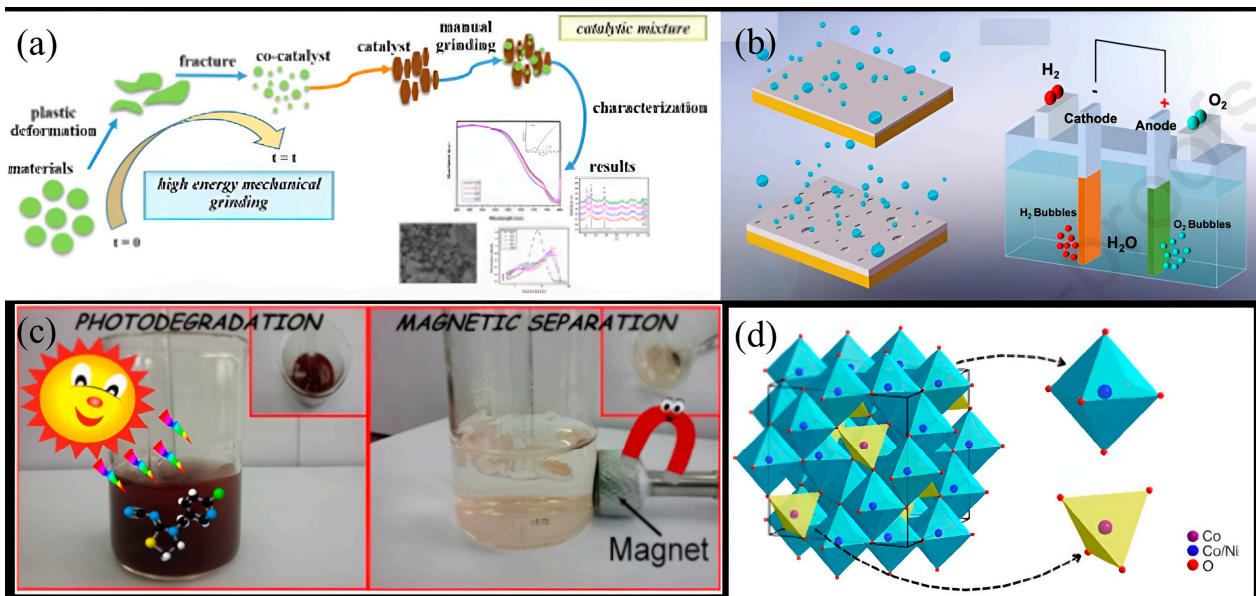
Figure 4. (**a**–**c**) Catalyst mechanisms and functions, (**d**) structure diagram [49–61]. (**a**) Reprinted from Fuel, 5416481031506 [54], Copyright (2022), with permission from Elsevier. (**b**) Reprinted from Applied Surface Science, 54164800925859 [49], Copyright (2022), with permission from Elsevier. (**c**) Reprinted from Journal of Industrial and Engineering Chemistry, open access [44], Copyright (2022). (**d**) Reprinted from Journal of Zhejiang University-Science A, 5416481031506 [56], Copyright (2022), with permission from Elsevier.

Table 1. Comparison of catalytic hydrogen evolution performance of Ni-Co alloy and its composites [51–61].

Number	Catalyst	Structure	At 10 mA·cm^{-2} Overpotential	Electrolyte Solution
1	Nickel-cobalt-titanium alloy	Electrodeposited films	125 mV	Alkaline solution
2	Ni-Co-(WC)$_{40}$	A net skeleton with small particles	135 mV	0.5 M H$_2$SO$_4$
3	Ni-Co-(WC)$_{30}$	A net skeleton with small particles	140 mV	0.5 M H$_2$SO$_4$
4	Ni-Co-(WC)$_{20}$	A net skeleton with small particles	160 mV	0.5 M H$_2$SO$_4$
5	Ni-Co-(WC)$_{10}$	A net skeleton with small particles	210 mV	0.5 M H$_2$SO$_4$
6	Ni-Co alloy	Smooth net skeleton	250 mV	0.5 M H$_2$SO$_4$
7	Ni-Co alloy	Porous form	54 mV	1 M KOH
8	Nickel/cobalt hydroxide nanoflakes/C	Nanopatches	39 mV	1 M NaOH
9	NiCo$_2$O$_4$@Ni$_2$P/NAs	Nanowire	141 mV	1 M KOH
10	NiCo$_2$O$_4$/NAs	Nanorods	315 mV	1 M KOH
11	Ni$_2$P/NAs	nanoparticle	210 mV	1 M KOH
12	NiCo$_2$O$_4$@Ni$_2$P/NAs	Nanowire	116 mV	0.5 M H$_2$SO$_4$
13	Co$_3$Fe$_7$@NCNTFs	Porous pipe	264 mV	1 M KOH
14	NiCoO$_2$@C	Wormlike	51 mV	1 M KOH
15	CoMoS$_4$/NF	nanoparticle	256 mV	1 M NaOH
16	NiCo$_2$S$_4$@δ-MnO$_2$/NF	Cactus-shaped	114 mV	1 M KOH
17	NiCo$_2$S$_4$/NF	Cactus-shaped	126 mV	1 M KOH
18	δ-MnO$_2$/NF	Cactus-shaped	135 mV	1 M KOH

4. Magnetic Nano Wave-Absorbing Materials

In recent years, with the wide use of electronic and wireless technology, electromagnetic pollution has become a new problem facing mankind. The absorption and shielding

of electromagnetic waves are also of great significance to military and national defense. Microwave-absorbing materials play an important role in radar monitoring and shielding. Therefore, for human safety, we need to reduce electromagnetic pollution and enhance the performance of microwave-absorbing materials. The commonly used microwave-absorbing materials are dielectric and electromagnetic. In order to improve their properties, a new system of composite powders has been developed, including hard magnetic and soft magnetic materials. The main parameters for evaluating electromagnetic wave-absorbing materials are impedance matching and dissipation capacity. Impedance matching requires that electromagnetic waves are absorbed by the materials as much as possible without being reflected. Dissipation capacity shows the consumption capacity of electromagnetic wave-absorbed materials [62,63].

Most of the existing microwave-absorbing materials are carbon-based, such as carbon nanotubes, graphite carbon, and carbon balls. In order to improve the ability of microwave-absorbing materials, researchers have proposed carbon materials compounded with transition metals. Iron, nickel, cobalt, and their oxides have high permeability, which combines with the dielectric properties of carbon materials. These are new types of microwave-absorbing materials, which can dissipate electromagnetic waves and adjust impedance matching [64–67].

Given this, Sachin et al. [68] prepared a $BaFe_{12}O_{19}/NiFe_2O_4$ microwave-absorbing material by chemical coprecipitation and studied the effects of heat treatment temperature on the magnetic properties and reflection loss of $BaFe_{12}O_{19}/NiFe_2O_4$ nanoparticles. The saturation magnetization M_S of $BaFe_{12}O_{19}/NiFe_2O_4$ nanoparticles is related to high temperature, and it can be observed that with the increase of temperature, M_s increases from 1.045 emu/g to 55.188 emu/g. By evaluating the reflection loss of $BaFe_{12}O_{19}/NiFe_2O_4$ nanoparticles, it can be observed that the reflection loss of "synthetic" $BaFe_{12}O_{19}/NiFe_2O_4$ nanoparticles is very small, while the reflection loss of annealed $BaFe_{12}O_{19}/NiFe_2O_4$ nanoparticles is generally increased, and the reflection loss increases with the annealing temperature, which is due to the increase in the formation of $BaFe_{12}O_{19}/NiFe_2O_4$ nanoparticles. The improvement of reflection loss is a result of the formation of hard ferrite and soft ferrite, which can be explained by the exchange coupling interaction between hard magnetic ($BaFe_{12}O_{19}$) and soft magnetic ($NiFe_2O_4$) phases. Mu et al. [69] synthesized a $NiCo_2O_4$ material with excellent microwave absorption by adjusting the pH value. The pH value causes the structural change of $NiCo_2O_4$ material, thus improving its properties. Dielectric loss is the main mechanism for materials to absorb electromagnetic waves. The dielectric loss mainly comes from the polarization process, dielectric relaxation, and conduction loss. The relaxation phenomenon is caused by the agglomeration of the layered structures. The uneven interlayer gap enhances the interface polarization between the $NiCo_2O_4$ material and air, and the oxygen vacancy further enhances the dipole polarization to improve the dielectric loss. The impedance matching Z value closer to 1 means that when the electromagnetic wave reaches the surface of the absorbing material, most of the electromagnetic wave will penetrate the absorbant. Only a small part is reflected to maximize the function of the absorbant. Dielectric loss and impedance matching play an important role in microwave-absorbing materials. Zhao et al. [70] studied the effects of the Ni/Co content ratio on the morphology and properties of the Ni-Co-P nanoalloy. The results showed that the nanosheet can effectively prevent electromagnetic wave superposition. Due to the soft magnetic properties of the Ni-Co-P nanoalloy, the external electromagnetic wave can be quickly converted into heat energy during magnetic field magnetization to attenuate the electromagnetic wave. The attenuation degree is calculated by the reflection loss rate.

Figure 5a,b present two kinds of magnetic nanomaterials and illustrate the absorption mechanism of magnetic nanomaterials, providing a reference for the mechanism of other microwave-absorbing materials. Figure 5c shows the relationship between the complex permittivity, complex permeability, and frequency of the $NiCo_2O_4$ material, illustrating the electromagnetic absorption properties of the material. The absorption characteristics of electromagnetic waves are affected by the complex permittivity and permeability of the

material. The real part is related to energy storage and the imaginary part represents energy dissipation. The real part and imaginary part together determine the electromagnetic wave absorption performance of the absorber. It can be inferred from the figure that the absorber contributes little to the electromagnetic wave loss. The tangent of the magnetic loss proves this conclusion. The magnetic loss is close to constant 0, which indicates that the magnetic loss ability of these samples is poor. Therefore, dielectric loss is the main mechanism of the synthesis of $NiCo_2O_4$ by chemical coprecipitation in this work [67–77].
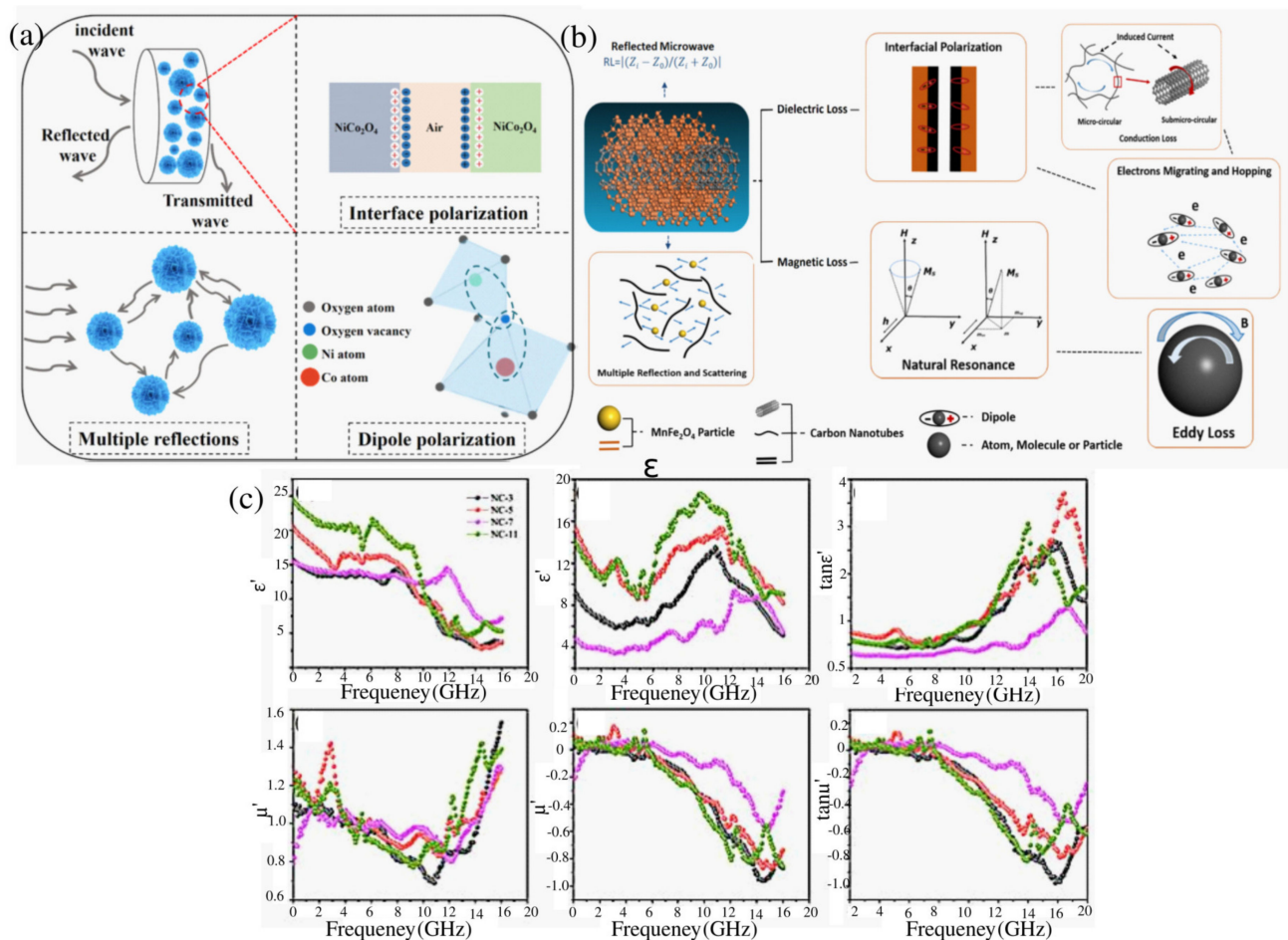

Figure 5. (**a**–**c**) Radar absorbing material performance characterization and radar absorbing mechanism [63,70]. (**a**,**c**) Reprinted from Journal of Materials Science, 5416520919952 [70], Copyright (2022), with permission from Elsevier. (**b**) Reprinted from Diamond and Related Materials, 5416520919952 [63], Copyright (2022), with permission from Elsevier.

The complex permittivity and permeability of absorbing materials are also important parameters of electromagnetic wave absorption characteristics. Their real part reflects the polarization and magnetization of materials under electromagnetic waves, and their imaginary part reflects the attenuation caused by the rearrangement of electromagnetic coupling torque under the influence of electromagnetic waves. The absorbing properties and the mechanism of absorbing materials are often related to their structure and morphology, which is the focus of the study of absorbing materials. At present, there are relatively few studies of nanometals as microwave-absorbing materials. The existing studies mainly focus on carbon materials, such as graphene, carbon nanotubes, and other materials. The nanometal materials and nano microwave-absorbing composites have better performance [71–77].

5. Electromagnetic Nanomaterials

Electromagnetic materials are widely used and affect people's lives and safety. Considering the rapid consumption of chemical fuels and the increasingly serious environmental pollution, people must constantly develop advanced technologies related to electric energy storage. The problem of radiation pollution is becoming more and more serious. Low-density, flexible, and high-performance electromagnetic interference (EMI) shielding materials are urgently needed. Magnetic nanomaterials with intrinsic conductivity and magnetism are good candidates for EMI shielding. Therefore, we must first understand the influencing factors and parameters of the electrical and magnetic properties of nanomaterials to have a basis before we can improve the electrical and magnetic properties of nanomaterials [78–80].

Dong et al. [81] prepared transition metal oxalate using the coprecipitation method and studied the quantitative effects of transition metal components on product nucleation and growth. The transition metal oxalate is used as the precursor of the battery and its surface activation energy was studied to improve the reasonable prediction and control of battery nanomaterials and other materials. The apparent activation energy is calculated as follows [82]:

$$ln(\tau) = -ln(A) + \frac{E}{kBT} \tag{2}$$

Here, A is the pre-exponential constant, E is the apparent activation energy, and kB is the Boltzmann constant. Linear fitting $ln(\tau)$ corresponds to the slope of $1/T$, and the values of E/kB and E are generated. E is the apparent activation energy under these solution conditions.

The conductivity of the nanomaterials is calculated as:

$$\sigma = \frac{1}{tR_S} \tag{3}$$

Here, σ, R_S, and t represent DC conductivity, sheet resistance, and sheet thickness, respectively.

Guo et al. [83] studied the preparation and photoelectrochemical properties of antimony-doped tin oxide nanomaterials using two modified coprecipitation methods. One is the precipitation-modified coprecipitation (PMC), the other is the solution-modified coprecipitation (SMC). The influencing factors and mechanisms of morphology, grain size, structure, and photoelectrochemical properties of antimony-doped tin oxide nanomaterials (ATO NPs) prepared by the two methods were studied. The main purpose was to reduce the resistivity of ATO NPs through the change of preparation process factors and to find the relationship between grain size and electrical properties. When the doping of Sb makes the Fermi level enter the conductive band of SnO_2, the electrical properties are improved, and the band gap is widened. This enlarged the optical band gap E_g. The changing trend of E_g is inconsistent with the changing trend of resistivity, indicating that the electrical properties of ATO NPs must be affected by other factors, and the E_g of ATO NPs has no obvious relationship with the electrical properties. In summary, the change of resistivity can be estimated by the morphology of ATO NPs. The electrical properties of ATO NPs prepared by the solution method are mainly affected by the uniform Sb doping, and effective Sb doping is affected by the concentration of HNO_3 and ethanol. Therefore, the PMC method should reduce scattering and increase mobility, and the optimal SMC method is Sb doping efficiency. Li et al. [84] prepared Ni-Co oxide/CNTs (carbon nanotubes) nanocomposites. The results show that Ni-Co oxide/CNTs nanocomposites have good electrical properties and energy storage capacity. The addition of CNTs reduces the size of Ni-Co oxide, while smaller metal oxide nanoparticles modify CNTs. These show better electrical properties due to the increase of their active centers and specific surface area. At the same time, after mixing Ni-Co oxide with CNTs, Ni-Co oxide covers the surface of CNTs, making the surface of CNTs rough. The gap between porous nanoparticles is conducive to energy storage.

Yan et al. [73] studied the effects of Ni and Co content on the morphology and magnetic properties of Ni-Co composites. The Co leaf metal microspheres have higher saturation magnetization M_S and coercive force H_C than Ni metal microspheres. The high M_S of Co leaf metal microspheres comes from the higher atomic magnetic moment of Co, and the coercive force is proportional to the anisotropic field N_A. Co-leaf metal microspheres have FCC and HCP structures. Therefore, it has a higher magnetocrystalline anisotropy field than FCC Ni metal microspheres. Co leaf metal microspheres are composed of nanoflakes, which have a higher shape anisotropy field than spherical ones, meaning that Co leaf metal microspheres have higher H_A. Therefore, Co leaf metal microspheres have higher H_C.

Figure 6a depicts a P@Ni-Co-120 hybrid film prepared by chemical coprecipitation and a combination of several methods, which is thicker than the 12 EMI shielding materials reported by most. PAN-PU nanofiber film coated with Ni-Co alloy nanoparticles is a thinner and lighter electromagnetic interference shielding material with low preparation cost and high shielding properties. Figure 6b is the shielding mechanism diagram of the P@Ni-Co-120 hybrid film. Figure 6c shows that the layered structure has an important effect on electromagnetic materials [73,78–87].
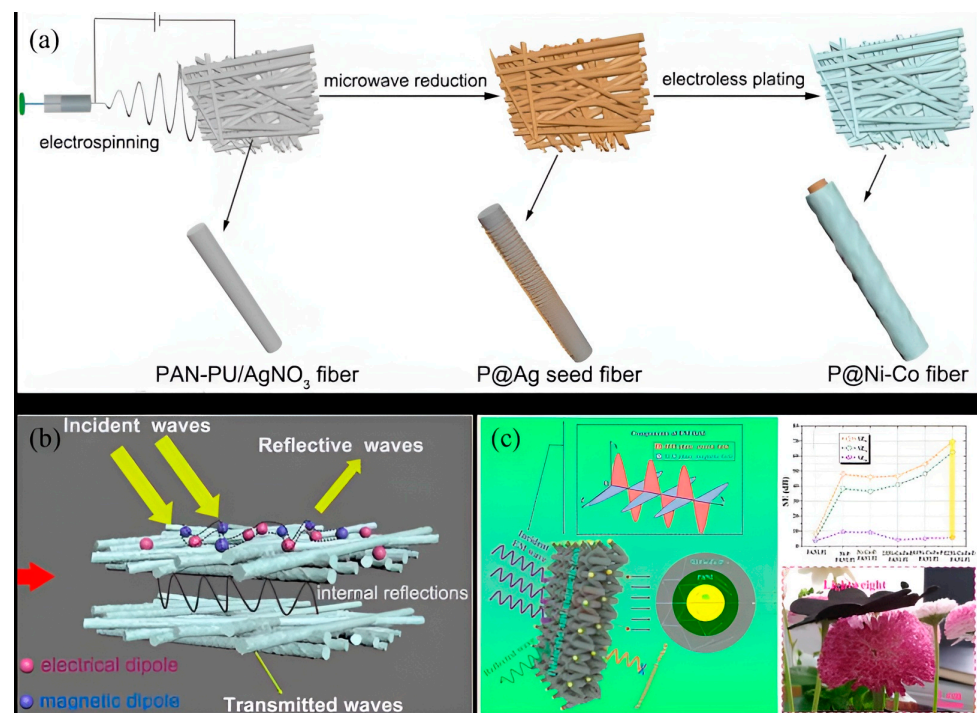

Figure 6. The preparation process and mechanism of magnetic absorbing materials [82,83]. (**a**,**b**) Reprinted from Journal of Alloys and Compounds, 5416500493658 [78], Copyright (2022), with permission from Elsevier. (**c**) Reprinted from Chemical Engineering Journal, 5416510964395 [77], Copyright (2022), with permission from Elsevier.

Because the density and thickness of EMI shielding materials are very important for EMI shielding characteristics, magnetic nanomaterials prepared by chemical coprecipitation are generally layered structures. Hence, the chemical coprecipitation method is suitable for the preparation of nanoelectromagnetic materials. The layer structure of magnetic nanomaterials prepared by chemical coprecipitation combined with electrodeposition or electroless plating is beneficial to electromagnetic properties. The electrical properties of nanomaterials are mainly reflected in the use of materials such as battery electrodes or capacitors and other electrical devices. There are also a variety of nanomagnetic materials, mainly nano iron, cobalt, nickel, and their alloys and composites, which are widely used. Doping nanometal particles and composites are effective ways to improve electrical and magnetic properties.

The structure and morphology of materials are also important factors affecting electrical and magnetic properties, which is also the focus of current research [73,82,85–87].

6. Magnetic Nano Adsorbents

In modern society, dye wastewater not only exists in the industry but is also used by other industries. Therefore, to purify wastewater, it is necessary to degrade dyes and purify water sources. Generally, the adsorption method is used. Therefore, it is necessary to understand the factors affecting adsorption to actively regulate and complete water treatment and other related issues in the treatment process. Carbon-based materials are good adsorption materials, and their adsorption capacity can be greatly improved by compounding with magnetic metal materials. Therefore, in recent years, composite carbon and magnetic metal materials have been widely used [88–93].

Rachida et al. [94] prepared Zn-Fe layered double hydroxides to catalyze the degradation of carmine in an aqueous solution. By using the chemical coprecipitation method, Zn-Fe-LDH nanomaterials were prepared under the conditions of constant pH (slowly adding pH agent to keep the pH unchanged), variable pH (slowly adding pH agent), and direct coprecipitation (rapidly adding pH agent). They studied the effects of the initial concentration of carmine dye, reaction temperature, the dosage of adsorbent Zn-Fe-LDH nanomaterials, contact time, and pH on dye removal by adsorption, and determined the best conditions for dye removal. The results showed that in the initial stage, the adsorption sites had not been consumed, so there were many adsorption sites and the adsorption rate was fast. The more adsorbent was used, the better the removal effect was. A higher temperature is favorable for adsorption. After 40 min, 50 min, and 80 min, the removal rates of carmine dye in Zn-Fe-LDH prepared by constant pH coprecipitation, direct coprecipitation, and constant pH coprecipitation were 96.74%, 95.7%, and 92.48%, respectively. Zhang et al. [95] studied the adsorption and removal of phenanthrene in water by magnetic multi-wall carbon nanotubes (MMWCNT), magnetic single-wall carbon nanotubes (MSWCNT), and magnetic graphene nanosheets (MGN). The results show that pH value has little effect on the removal rate of phenanthrene, and the adsorption effect is better under weak acid conditions. Wang et al. [91] discussed the relationship between the structural properties of magnetic ZrO_2/Fe_3O_4 nanocomposites and their phosphate adsorption capacity in detail. The results showed that the phosphate adsorption capacity of adsorbents was closely related to their specific surface area and surface hydroxyl groups.

Magnetic nanomaterials are the main materials for water pollution treatment and water environmental remediation. The main disadvantage of magnetic nanomaterials is that they are easy to aggregate and accumulate, which leads to the blockage of the adsorption sites of magnetic nanomaterials. In order to solve this problem, the functionalization can be enhanced by improving the dispersion, extraction efficiency, and selectivity of the adsorbent to the target compound. In order to make magnetic nanomaterials widely used in industry, convenient and cheap preparation methods—such as chemical coprecipitation—have the advantages of high adsorption capacity, multi-cycle reuse, large active surface area, high chemical and mechanical durability, and simple operation. Figure 7 shows the magnetic extraction process in an aqueous solution for reference [90–103].

To summarize, adsorption treatment is a simple, economic, and easy separation method. The adsorption efficiency depends on parameters such as pH, temperature, and initial color. As a result, it is very important to optimize the influencing factors. There are many kinds of nanoadsorbents. In general, it can be analyzed by improving the dispersion of adsorbents, extraction efficiency, and selectivity to target compounds, and it can also enhance the function of nanoadsorbents. Nanoadsorption materials mainly include nanocarbon adsorption, nano-oxide adsorption, nanomagnetic material adsorption, etc. Nanomaterials have a large surface area, and a large number of microporous channels are required inside the adsorption materials to increase the adsorption capacity, thus the adsorption materials need a large specific surface area. Accordingly, nanomagnetic

materials have superior adsorption capacity and can be used to treat various wastewater and extract metals, which are widely used in the food industry [97–103].
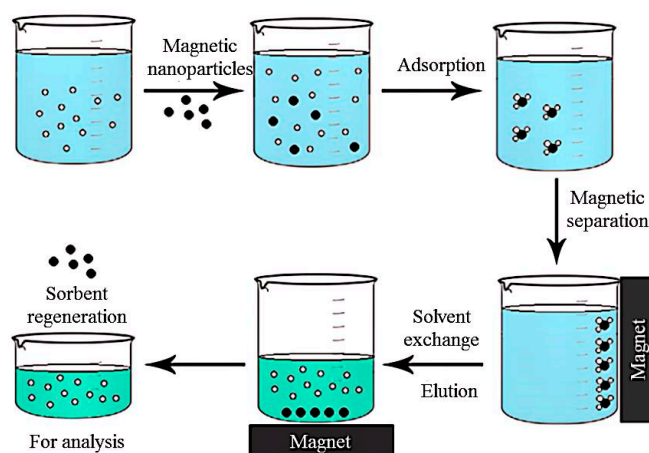

Figure 7. Steps of magnetic extraction in water environment [103]. Reprinted from Applied Science, open access, Copyright (2022).

7. Conclusions

The chemical coprecipitation process is simple and suitable for large-scale industrial applications. At present, the chemical coprecipitation method has been widely used to prepare nanomaterials. The conditions for the preparation of nanomaterials by the chemical coprecipitation method are controllable and can usually be prepared in one step, which is very important for the application of the chemical coprecipitation method. Nanomaterials also play an important role in today's society, such as in aerospace, military fields, magnetic materials, the battery industry, etc. By summarizing the preparation of nanomaterials by chemical coprecipitation, it can be seen that the research on the preparation of nanomaterials must mainly explore factors that will affect the morphology, structure, size, and related properties of nanomaterials, which are the key in the preparation of nanomaterials. It is easy to agglomerate when preparing nanomaterials by chemical coprecipitation. This is the main reason that the addition of precipitant makes the local concentration rise rapidly and agglomerates occur. Therefore, it is a common problem to explore the ways of adding precipitants to reduce agglomeration.

Magnetic nanomaterials are widely used because of their high saturation magnetization, high coercive force, stability, and dispersion. At present, there are dozens of elements used in magnetic nanomaterials, including metals and their oxides, alloys, and so on. With the development of nanotechnology, the application range of magnetic nanomaterials has been greatly improved. For example, magnetic nanomaterials with high permeability, low loss, and high saturation magnetization are widely used in transformer materials, sensor devices, and so on. As biomaterials, magnetic nanoparticles are also a hot research topic in biomedicine, and some of them have already been used. Magnetic nanomaterials have broad application prospects in various fields such as electronics, mechanics, optics, magnetism, chemistry, and biology. Therefore, the summary and prospects are as follows.

1. The structure and morphology of magnetic nanomaterials have a strong impact on their magnetic properties, and HCP materials have a higher magnetocrystalline anisotropy field than FCC and BCC structure materials. Therefore, the HCP materials have high coercivity. The larger the aspect ratio, the higher the shape anisotropy field and the greater the saturation magnetization of the materials.
2. The magnetic properties of magnetic nanomaterials are their basic properties. In order to improve their magnetic properties, carbon materials and transition metal composites are effective measures, and two-dimensional structures and mesoporous

structures are also measured to change their magnetic properties. Their properties are related to the application of magnetic nanomaterials.

3. Magnetic nanomaterials play an important role in various fields. For example, in biomedicine, most of the current research is focused on the study of targeted drugs, magnetic hyperthermia, etc. Therefore, one can extend the targeting of magnetic nanomaterials to more drugs and understand the effect of magnetic nanomaterials on drugs and their toxicity to organisms.

4. One can systematically and specifically analyze the factors that affect the properties and applications of magnetic nanomaterials, such as specific surface area, the influence of magnetic properties, structure and morphology of the properties, and applications of magnetic nanomaterials. For instance, when magnetic nanomaterials are used as catalysts, their catalytic activity can be predicted when their size, structure, and magnetic properties reach a certain level.

Author Contributions: Methodology, F.Y. (Fan Yang); software, P.H.; validation, G.C.; formal analysis, F.Z.; investigation, L.G.; resources, A.A.V.; data curation, S.G.; writing—original draft preparation, Z.L.; writing—review and editing, Y.S.; project administration, K.W.; funding acquisition, F.Y. (Fei Yin). All authors have read and agreed to the published version of the manuscript.

Data Availability Statement: Data supporting the findings of this study are available within the article.

Conflicts of Interest: The authors declare no conflict of interest.

References

1. Ancira-Cortez, A.; Morales-Avila, E.; Ocampo-García, B.E.; González-Romero, C.; Medina, L.A.; López-Téllez, G.; Cuevas-Yáñez, E. Preparation and Characterization of a Tumor-Targeting Dual-Image System Based on Iron Oxide Nanoparticles Functionalized with Folic Acid and Rhodamine. *J. Nanomater.* **2017**, *2017*, 5184167. [CrossRef]

2. Kooti, M.; Nasiri, E. Synthesis of a novel magnetic nanocatalyst based on rhodium complex for transfer hydrogenation of ketone. *Appl. Organomet. Chem.* **2019**, *33*, e4886. [CrossRef]

3. Zhao, X.F.; Wang, W.Y.; Li, X.D.; Li, S.P.; Song, F.G. Core-shell structure of Fe_3O_4@MTX-LDH/Au NPs for cancer therapy. *Mater Sci. Eng. C Mater. Biol. Appl.* **2018**, *89*, 422–428. [CrossRef] [PubMed]

4. Jesus, A.C.B.; Jesus, J.R.; Lima, R.J.S.; Moura, K.O.; Almeida, J.M.A.; Duque, J.G.S.; Meneses, C.T. Synthesis and magnetic interaction on concentrated Fe_3O_4 nanoparticles obtained by the co-precipitation and hydrothermal chemical methods. *Ceram. Int.* **2020**, *46*, 11149–11153. [CrossRef]

5. Jiang, L.P.; Zhu, Y.L.; Yang, Q.B. Preparation of novel magnetic nano-composite microgel adsorbent and its application. *Ind. Water Treat.* **2018**, *38*, 04422.

6. Lei, Y.M.; Xiao, B.Q.; Liang, W.B.; Chai, Y.Q.; Yuan, R.; Zhuo, Y. A robust, magnetic, and self-accelerated electrochemiluminescent nanosensor for ultrasensitive detection of copper ion. *Biosens. Bioelectron.* **2018**, *109*, 109–115. [CrossRef] [PubMed]

7. Dehkordi, S.S.S.; Albadi, J.; Jafari, A.A.; Samimi, H.A. Catalytic study of the copper-based magnetic nanocatalyst on the aerobic oxidation of alcohols in water. *Res. Chem. Intermed.* **2021**, *47*, 2527–2538. [CrossRef]

8. Najafinejad, M.S.; Mohammadi, P.; Afsahi Mehdi, M.; Sheibani, H. Biosynthesis of Au nanoparticles supported on Fe_3O_4@polyaniline as a heterogeneous and reusable magnetic nanocatalyst for reduction of the azo dyes at ambient temperature. *Mater. Sci. Eng. C Mater. Biol. Appl.* **2019**, *98*, 19–29. [CrossRef]

9. Amir, M.; Kurtan, U.; Baykal, A. Synthesis and application of magnetically recyclable nanocatalyst Fe_3O_4@NiCo@Cu in the reduction of azo dyes. *Chin. J. Catal.* **2015**, *36*, 1280–1286. [CrossRef]

10. Gil, S.; Correia, C.R.; Mano, J.F. Magnetically labeled cells with surface-modified Fe_3O_4 spherical and rod-shaped magnetic nanoparticles for tissue engineering applications. *Adv. Healthc. Mater.* **2015**, *4*, 883–891. [CrossRef]

11. Zhang, H.; Dai, Y.M.; Liu, L.M. Novel monolayer pyrite FeS_2 with atomic-thickness for magnetic devices. *Comput. Mater. Sci.* **2015**, *101*, 255–259. [CrossRef]

12. Li, W.; Yang, Z.Y.; Hou, Y.L.; Gao, S. Controllable synthesis and magnetic regulation of two-dimensional magnetic nanomaterials. *Prog. Chem.* **2020**, *32*, 1437–1451.

13. Ye, M.F.; Lu, Y.F.; Dong, Q.; Huang, X.J.; Xu, L.X. Preparation and Application of Fe_3O_4 Nanomaterials. *Chin. Ceram.* **2014**, *50*, 12.

14. Shan, A.X.; Wang, R.M. Progress of the Research on Controllable Synthesis and Mesoscopic Properties for Magnetic Nanomaterials. *Mater. China* **2016**, *35*, 292–301.

15. Šuljagić, M.; Vulić, P.; Jeremić, D.; Pavlović, V.; Filipović, S.; Kilanski, L.; Lewinska, S.; Slawska-Waniewska, A.; Milenković, M.R.; Nikolić, A.S.; et al. The influence of the starch coating on the magnetic properties of nanosized cobalt ferrites obtained by different synthetic methods. *Mater. Res. Bull.* **2021**, *134*, 111117. [CrossRef]

16. Shao, H.; Wang, L.; Lin, T.; Zhang, Y.; Zhang, Z. Effect of protamine on Fe_3O_4@CS@GFTN composite magnetic nanoparticles. *Funct. Mater. Lett.* **2019**, *13*, 2050001. [CrossRef]

17. Kılıç, M.; Kahya, N.D.; Mısırlıoğlu, B.S.; Çakır, Ö.; Özdemir, Z.G. Dielectric and magnetic properties of $CuFe_2O_4$/CuO nanocomposites. *Ferroelectrics* **2021**, *571*, 183–199. [CrossRef]

18. Zhang, Y.L. Porous Fibrous Fe-Ni Alloy Powders Were Prepared by Coordination Coprecipitation Thermal Decomposition Reduction Method. Ph.D. Thesis, Central South University, Changsha, China, 2009.

19. Hashimoto, M.; Takahashi, S.; Kawahara, K.; Ogawa, T.; Kawashita, M. Effect of heating conditions on the magnetic properties of micron-sized carboxyl modified-magnetite particles synthesized by a spray pyrolysis and heating process. *Adv. Powder Technol.* **2022**, *33*, 103412. [CrossRef]

20. Sidhureddy, B.; Prins, S.; Wen, J.; Thiruppathi, A.R.; Govindhan, M.; Chen, A. Synthesis and Electrochemical Study of Mesoporous Nickel-Cobalt Oxides for Efficient Oxygen Reduction. *ACS Appl. Mater. Interfaces* **2019**, *11*, 18295–18304. [CrossRef]

21. Liu, H.L.; Lin, C.B.; Chen, Y. Research Progress of Long Chain Conjugated Schiff Base Absorbing Materials. *Mater. Guide A Over-View* **2012**, *26*, 7.

22. Tyagi, S.; Pandey, V.S.; Goel, S.; Garg, A. Synthesis and characterization of RADAR absorbing $BaFe_{12}O_{19}$/$NiFe_2O_4$ magnetic nano-composite. *Integr. Ferroelectr.* **2018**, *186*, 25–31. [CrossRef]

23. Chen, M.J.; Zhang, H.C.; Guan, Z.R. Research on Structural and Magnetic Features of Fe_3O_4 Nanoparticles Synthesized by Chemical Co-Precipitation Method. *Mater. Guide* **2008**, *22*.

24. Zhang, W.X.; Li, H.T.; Lu, X. Preparation of oil-soluble Fe_3O_4 nanoparticles by chemical coprecipitation. *China Powder Technol.* **2015**, *4*.

25. Hu, W.Z.; Hong, Y. Preparation of Fe_3O_4 nanoparticles by chemical coprecipitation method and its application in magnetic particle detection. *Spec. Equip. Saf. Technol.* **2019**, *3*, 2.

26. Li, Y.; Hu, K.; Chen, B.; Liang, Y.; Fan, F.; Sun, J.; Zhang, Y.; Gu, N. Fe_3O_4@PSC nanoparticle clusters with enhanced magnetic properties prepared by alternating-current magnetic field assisted co-precipitation. *Colloids Surf. A Physicochem. Eng. Asp.* **2017**, *520*, 348–354. [CrossRef]

27. Zhan, H.; Bian, Y.H.; Yuan, Q. Preparation and Potential Applications of Super Paramagnetic Nano-Fe_3O_4. *Processes* **2018**, *6*, 33. [CrossRef]

28. Ignatovich, Z.; Novik, K.; Abakshonok, A.; Koroleva, E.; Beklemisheva, A.; Panina, L.; Kaniukov, E.; Anisovich, M.; Shumskaya, A. One-Step Synthesis of Magnetic Nanocomposite with Embedded Biologically Active Substance. *Molecules* **2021**, *26*, 937. [CrossRef]

29. Egizbek, K.; Kozlovskiy, A.L.; Ludzik, K.; Zdorovets, M.V.; Korolkov, I.V.; Marciniak, B.; Chudoba, J.M.D.; Nazarova, A.; Kontek, R. Stability and cytotoxicity study of $NiFe_2O_4$ nanocomposites synthesized by co-precipitation and subsequent thermal annealing. *Ceram. Int.* **2020**, *46*, 16548–16555. [CrossRef]

30. Xiao, M.L.; Li, N.; Lv, S.S. Iron oxide magnetic nanoparticles exhibiting zymolyase-like lytic activity. *Chem. Eng. J. C* **2020**, *394*, 125000. [CrossRef]

31. Funnell, J.L.; Balouch, B.; Gilbert, R.J. Magnetic Composite Biomaterials for Neural Regeneration. *Front. Bioeng. Biotechnol.* **2019**, *7*, 179. [CrossRef]

32. Mohapatra, S.; Asfer, M.; Anwar, M. Carboxymethyl Assam Bora rice starch coated SPIONs: Synthesis, characterization and in vitro localization in a micro capillary for simulating a targeted drug delivery system. *Int. J. Biomacromol.* **2018**, *115*, 920–932. [CrossRef] [PubMed]

33. Forouzandehdel, S.; Forouzandehdel, S.; Rezghi Rami, M. Synthesis of a novel magnetic starch-alginic acid-based biomaterial for drug delivery. *Carbohydr. Res.* **2020**, *487*, 107889. [CrossRef] [PubMed]

34. Zheng, X.; Duan, F.; Song, Z.; Mo, H.; Li, Z.; Song, Y.; Su, Y.; Wang, X. A TMPS-designed personalized mandibular scaffolds with optimized SLA parameters and mechanical properties. *Front. Mater.* **2022**, *9*, 966031. [CrossRef]

35. Chen, L.; Zhong, H.; Qi, X.; Shao, H.; Xu, K. Modified core-shell magnetic mesoporous zirconia nanoparticles formed through a facile "outside-to-inside" way for CT/MRI dual-modal imaging and magnetic targeting cancer chemotherapy. *RSC Adv.* **2019**, *9*, 13220–13233. [CrossRef] [PubMed]

36. Zhou, S.; Sun, J.; Sun, L.; Dai, Y.; Liu, L.; Li, X.; Wang, J.; Weng, J.; Jia, W.; Zhang, Z. Preparation and characterization of interfer-on-loaded magnetic biodegradable microspheres. *J. Biomed. Mater. Res. B Appl. Biomater.* **2008**, *87*, 189–196. [CrossRef] [PubMed]

37. Mabrouk, M.; Abd El-Wahab, R.M.; Beherei, H.H.; Selim, M.M.; Das, D.B. Multifunctional magnetite nanoparticles for drug delivery: Preparation, characterization, antibacterial properties and drug release kinetics. *Int. J. Pharm.* **2020**, *587*, 119658. [CrossRef]

38. Schwaminger, S.P.; Blank-Shim, S.A.; Scheifele, I.; Fraga-Garcia, P.; Berensmeier, S. Peptide binding to metal oxide nanoparticles. *Faraday Discuss* **2017**, *204*, 233–250. [CrossRef]

39. Xiao, Q.; Liu, C.; Ni, H.; Zhu, Y.; Jiang, Z.; Xiao, A. beta-Agarase immobilized on tannic acid-modified Fe_3O_4 nanoparticles for efficient preparation of bioactive neoagaro-oligosaccharide. *Food Chem.* **2019**, *272*, 586–595. [CrossRef]

40. Huynh, H.L.; Tucho, W.M.; Yu, X.; Yu, Z. Synthetic natural gas production from CO_2 and renewable H_2: Towards large-scale production of Ni–Fe alloy catalysts for commercialization. *J. Clean. Prod.* **2020**, *264*, 121720. [CrossRef]

41. Azancot, L.; Bobadilla, L.F.; Santos, J.L.; Córdoba, J.M.; Centeno, M.A.; Odriozola, J.A. Influence of the preparation method in the met-al-support interaction and reducibility of Ni-Mg-Al based catalysts for methane steam reforming. *Int. J. Hydrogen Energy* **2019**, *44*, 19827–19840. [CrossRef]

42. Zheng, Y.S.; Qiu, S.; Deng, F.X. A charcoal-shaped catalyst $NiFe_2O_4/Fe_2O_3$ in electro-Fenton: High activity, wide pH range and catalytic mechanism. *Environ. Technol.* **2019**, *2456*, 1–32. [CrossRef]

43. Cui, W.; Liu, L.; Yang, J.; Tan, N. Effect of preparation method on the catalytic performance of formaldehyde oxidation over octahedral Fe_3O_4 microcrystals supported Pt catalysts. *J. Dispers. Sci. Technol.* **2019**, *41*, 1831–1838. [CrossRef]

44. Banić, N.D.; Abramović, B.F.; Krstić, J.B.; Šojić Merkulov, D.V.; Finčur, N.L.; Mitrić, M.N. Novel WO_3/Fe_3O_4 magnetic photocatalysts: Preparation, characterization and thiacloprid photodegradation. *J. Ind. Eng. Chem.* **2019**, *70*, 264–275. [CrossRef]

45. Zheng, Z.; Guo, Y.; Wan, H.; Chen, G.; Zhang, N.; Ma, W.; Liu, X.; Liang, S.; Ma, R. Anchoring Active Sites by Pt_2FeNi Alloy Nanoparticles on NiFe Layered Double Hydroxides for Efficient Electrocatalytic Oxygen Evolution Reaction. *Energy Environ. Mater.* **2021**, *5*, 270–277. [CrossRef]

46. Wu, D.D.; Zhong, S.; Wen, M. A Flower-cluster Heterogenous Structure Assembled by Ultrathin $NiCo/NiCoOx-SiO_2$ Nanobelts with Stable Catalytic Performance. *Colloids Surf. A Physicochem. Eng. Asp.* **2020**, *610*, 125590. [CrossRef]

47. Horoz, S.; Baytar, O.; Sahin, O.; Kilicvuran, H. Photocatalytic degradation of methylene blue with Co alloyed CdZnS nanoparticles. *J. Mater. Sci. Mater. Electron.* **2017**, *29*, 1004–1010. [CrossRef]

48. Wang, F.; Yang, H.; Zhang, H.M. Growth process and enhanced photocatalytic performance of $CuBi_2O_4$ hierarchical microcuboids decorated with Au-Ag alloy nanoparticles. *J. Mater. Sci. Mater. Electron.* **2018**, *29*, 1304–1316. [CrossRef]

49. Wang, J.; Shao, H.; Ren, S.; Hu, A.; Li, M. Fabrication of porous Ni-Co catalytic electrode with high performance in hydrogen evolution reaction. *Appl. Surf. Sci.* **2021**, *539*, 148045. [CrossRef]

50. Wen, Y.; Wei, Z.; Ma, C.; Xing, X.; Li, Z.; Luo, D. MXene Boosted CoNi-ZIF-67 as Highly Efficient Electrocatalysts for Oxygen Evolution. *Nanomaterials* **2019**, *9*, 775. [CrossRef]

51. Zheng, J. Seawater splitting for high-efficiency hydrogen evolution by alloyed PtNix electrocatalysts. *Appl. Surf. Sci.* **2017**, *413*, 360–365. [CrossRef]

52. Güy, N.; Atacan, K.; Karaca, E.; Özacar, M. Role of Ag_3PO_4 and Fe_3O_4 on the photocatalytic performance of magnetic $Ag_3PO_4/ZnO/Fe_3O_4$ nanocomposite under visible light irradiation. *Sol. Energy* **2018**, *166*, 308–316. [CrossRef]

53. Mousavi, M.; Nakhaei Pour, A.; Gholizadeh, M.; Mohammadi, A.; Kamali Shahri, S.M. Dry reforming of methane by $La_{0.5}Sr_{0.5}NiO_3$ perovskite oxides: Influence of preparation method on performance and structural features of the catalysts. *J. Chem. Technol. Biotechnol.* **2020**, *95*, 2911–2920. [CrossRef]

54. Alonso-Rodríguez, D.W.; Ruiz-Luna, H.; Alfaro-Cruz, M.R.; Bañuelos-Frias, A.; Alvarado-Perea, L.; Valero-Luna, C. Synthesis and characterization of $BaFe_{12}O_{19}$-WC catalysts prepared by mechanical milling. *Fuel* **2020**, *280*, 118608. [CrossRef]

55. Marsooli, M.A.; Fasihi-Ramandi, M.; Adib, K.; Pourmasoud, S.; Ahmadi, F.; Ganjali, M.R.; Sobhani Nasab, A.; Nasrabadi, M.R.; Plonska-Brzezinska, M.E. Preparation and Characterization of Magnetic $Fe_3O_4/CdWO_4$ and $Fe_3O_4/CdWO_4/PrVO_4$ Nanoparticles and Investigation of Their Photocatalytic and Anticancer Properties on PANC1 Cells. *Materials* **2019**, *12*, 3274. [CrossRef] [PubMed]

56. Fang, Y.Y.; Wang, X.Z.; Chen, Y.Q.; Dai, L.Y. $NiCo_2O_4$ nanoparticles: An efficient and magnetic catalyst for Knoevenagel condensation. *J. Zhejiang Univ.-Sci. A* **2020**, *21*, 74–84. [CrossRef]

57. Wang, Q.; Wang, H.; Cheng, X.; Fritz, M.; Wang, D.; Li, H.; Bund, A.; Chen, G.; Schaaf, P. $NiCo_2O_4@Ni_2P$ nanorods grown on nickel nanorod arrays as a bifunctional catalyst for efficient overall water splitting. *Mater. Today Energy* **2020**, *17*, 100490. [CrossRef]

58. Yuan, Q.; Yu, Y.; Sherrell, P.C.; Chen, J.; Bi, X. Fe/Co-based Bimetallic MOF-derived $Co_3Fe_7@NCNTFs$ Bifunctional Electrocatalyst for High-Efficiency Overall Water Splitting. *Chem. Asian J.* **2020**, *15*, 1728–1735. [CrossRef]

59. Kamali Moghaddam, S.; Ahmadian, S.M.S.; Haghighi, B. $NiCoO_2$-carbon composite as an efficient bifunctional catalyst for electrochemical water splitting. *Ionics* **2020**, *26*, 3959–3967. [CrossRef]

60. Yadav, A.A.; Hunge, Y.M.; Kang, S.-W. Highly efficient porous morphology of cobalt molybdenum sulfide for overall water splitting reaction. *Surf. Interfaces* **2021**, *23*, 101020. [CrossRef]

61. Zhang, R.; Huang, L.; Yu, Z.; Jiang, R.; Hou, Y.; Sun, L.; Zhang, B.; Huang, Y.; Ye, B.; Zhang, Y. Spherical cactus-like composite based on transition metals Ni, Co and Mn with 1D/2D bonding heterostructure for electrocatalytic overall water splitting. *Electrochim. Acta* **2019**, *323*, 134845. [CrossRef]

62. Meng, R.; Zhang, T.; Yu, H.; Zhang, J.; Wen, G.; Huang, X.; Huang, L.; Xia, L.; Zhong, B. A facile coprecipitation method to synthesize FexOy/Fe decorated graphite sheets with enhanced microwave absorption properties. *Nanotechnology* **2019**, *30*, 185704. [CrossRef]

63. Pang, H.; Sahu, R.P.; Duan, Y.; Puri, I.K. MnFe₂O₄-coated carbon nanotubes with enhanced microwave absorption: Effect of CNT content and hydrothermal reaction time. *Diam. Relat. Mater.* **2019**, *96*, 31–43. [CrossRef]
64. Zhao, Y.; Zhou, Z.; Chen, G.-X.; Li, Q. Coaxial double-layer-coated multiwalled carbon nanotubes toward microwave absorption. *Mater. Lett.* **2018**, *233*, 203–206. [CrossRef]
65. Wang, C.X.; Liu, Y.J. Development of magnetic loss absorbing materials. *Res. Technol.* **2021**, *58*.
66. Chen, G.H.; Zhou, F.L.; Zhao, L.P.; Duan, H.Z. Research progress on microwave absorbing mechanism and improving microwave absorbing properties of ferrite magnetic materials. *Prog. Chem. Eng.* **2015**, *34*, 3965–3969.
67. Ji, H.; Zhang, H.Y.; Wang, N.; Hong, X. Research Progress of Two Dimensional Carbide Ti₃C₂Tx/Magnetic Composite Wave Absorbing Materials. *Silk* **2021**, *58*, 33–39.
68. Cui, S.H.; Shen, X.D.; Yuan, L.S. Research Development of Electromagnetic Interference Shielding and Wave-Absorbing Materials. *Electron. Compon. Mater.* **2005**, *1*, 57–61.
69. Ye, Z.; Wang, K.; Li, X.; Yang, J. Preparation and characterization of ferrite/carbon aerogel composites for electromagnetic wave absorbing materials. *J. Alloys Compd.* **2022**, *893*, 162396. [CrossRef]
70. Mu, Y.; Zhang, L.; Liu, H.; Wu, H. Regulating pH value synthesis of NiCo₂O₄ with excellent electromagnetic wave absorbing performance. *J. Mater. Sci. Mater. Electron.* **2021**, *32*, 26059–26073. [CrossRef]
71. Zhao, S.; Wang, C.; Zhong, B. Optimization of electromagnetic wave absorbing properties for Ni-Co-P/GNs by controlling the content ratio of Ni to Co. *J. Magn. Magn. Mater.* **2020**, *495*, 165753. [CrossRef]
72. Luo, C.; Jiao, T.; Gu, J.; Tang, Y.; Kong, J. Graphene Shield by SiBCN Ceramic: A Promising High-Temperature Electromagnetic Wave-Absorbing Material with Oxidation Resistance. *ACS Appl. Mater. Interfaces* **2018**, *10*, 39307–39318. [CrossRef] [PubMed]
73. Yan, S.J.; Dai, S.L.; Ding, H.Y.; Wang, Z.Y.; Liu, D.B. Influence of Ni/Co molar ratio on electromagnetic properties and microwave absorption performances for Ni/Co paraffin composites. *J. Magn. Magn. Mater.* **2014**, *358–359*, 170–176. [CrossRef]
74. Chen, H.Q. Design and Synthesis of Nano-Metal Cobalt-Based/Carbon Composite Absorbing Materials. Master's Thesis, Harbin Institute of Technology, Harbin, China, 2015.
75. Feng, Y.; Yang, Y.; Wen, Q.; Riedel, R.; Yu, Z. Dielectric Properties and Electromagnetic Wave Absorbing Performance of Single-Source-Precursor Synthesized Mo₄.₈Si₃C₀.₆/SiC/C free Nanocomposites with an In Situ Formed Nowotny Phase. *ACS Appl. Mater. Interfaces* **2020**, *12*, 16912–16921. [CrossRef] [PubMed]
76. Ding, S.X.; Lu, M.; Zheng, G.K. Electromagnetic wave absorbing property of two-layer composite material. *Ordnance Mater. Sci. Eng.* **2016**, *39*, 88–91. [CrossRef]
77. Wang, Y.; Wang, W.; Ding, X.; Yu, D. Multilayer-structured Ni-Co-Fe-P/polyaniline/polyimide composite fabric for robust electromagnetic shielding with low reflection characteristic. *Chem. Eng. J.* **2020**, *380*, 122553. [CrossRef]
78. Zhang, N.; Zhao, R.; He, D.; Ma, Y.; Qiu, J.; Jin, C.; Wang, C. Lightweight and flexible Ni-Co alloy nanoparticle-coated electrospun polymer nanofiber hybrid membranes for high-performance electromagnetic interference shielding. *J. Alloys Compd.* **2019**, *784*, 244–255. [CrossRef]
79. Gurevich, S.Y.; Petrov, Y.V. Laser generation and electromagnetic detection of normal acoustic waves in ferromagnetic metals. *Tech. Phys.* **2016**, *61*, 432–435. [CrossRef]
80. Huang, X.; Dai, B.; Ren, Y.; Xu, J.; Zhu, P. Preparation and Study of Electromagnetic Interference Shielding Materials Comprised of Ni-Co Coated on Web-Like Biocarbon Nanofibers via Electroless Deposition. *J. Nanomater.* **2015**, *2015*, 320306. [CrossRef]
81. Ding, J.; Xu, H.; Chen, X. Facile hydrothermal synthesis of ternary Ni-Co-Se/carbon nanotube nanocomposites as advanced electrodes for lithium storage. *RSC Adv.* **2018**, *8*, 28710–28715. [CrossRef]
82. Kotel'nikova, S.V.; Suslonov, V.V.; Bobrysheva, N.P.; Osmolowsky, M.G.; Osmolowskaya, O.M. Synthesis of bimetallic nanoparticles based on cobalt and nickel. Effects of their composition and structure on catalytic and magnetic properties. *Russ. J. Gen. Chem.* **2017**, *87*, 1093–1094. [CrossRef]
83. Guo, Y.U.; Liu, S.; Liang, D.; Wang, Z.; Jiang, W.; Liu, C.; Wang, H.; Wang, N.A.N.; Ding, W.; Wang, L.I.; et al. Preparation and Electrical Properties of Antimony-Doped Tin Oxide Nanoparticles by Two Various Modified Coprecipitation Methods. *Surf. Rev. Lett.* **2019**, *27*, 1950176. [CrossRef]
84. Li, M.; Feng, W.; Su, W.; Song, C.; Cheng, L. MOF-derived hollow cage Ni-Co mixed oxide/CNTs nanocomposites with enhanced electrochemical performance for lithium-sulfur batteries. *Ionics* **2019**, *25*, 4037–4045. [CrossRef]
85. Dong, H.; Gardner, E.; Barron, A.F.; Koenig, G.M. Apparent activation energy of multicomponent transition metal oxalates to probe synthesis of battery precursor materials. *Powder Technol.* **2019**, *354*, 158–164. [CrossRef]
86. Zhao, X.; Ma, L.; Shen, X. Co-based anode materials for alkaline rechargeable Ni/Co batteries: A review. *Mater. J. Chem.* **2012**, *22*, 277–285. [CrossRef]
87. Couto, G.G.; Klein, J.J.; Schreiner, W.H.; Mosca, D.H.; De Oliveira, A.J.; Zarbin, A.J. Nickel nanoparticles obtained by a modified polyol process: Synthesis, characterization, and magnetic properties. *J. Colloid Interface Sci.* **2007**, *311*, 461–468. [CrossRef]
88. Hu, P.; Chen, Z.-Y.; Chang, T.; Deng, J.; Yang, F.; Wang, K.-S.; Li, Q.-W.; Hu, B.-L.; Yu, H.-L.; Wang, W.-P. Magnetic properties of the nanoscale coral-shaped Ni-Co alloy powder with different Co contents. *J. Alloys Compd.* **2017**, *727*, 332–337. [CrossRef]
89. Shao, L.; Sheng, L.; Wen, F.; Ying, Z.; Huang, H.; Zheng, P.; Wu, W. Enhanced electromechanical response and piezoelectric properties in lead-free erbium-modified Ba(Zr,Ti)O₃ piezoceramics. *Ceram. Int.* **2018**, *44*, 9915–9922. [CrossRef]
90. Ren, H.X.; Li, B.J.; Yu, Z.Y. Progress in preparation and application of common magnetic nano-adsorbent materials. *Shandong Jianzhu Univ.* **2017**, *32*, 7.

91. Ma, W.S.; Zhang, R.; Jiang, J.J. Research progress of nano-adsorption materials in the treatment of emerging pollutants. *Ind. Water Wastewater* **2016**, *47*, 7.
92. Nithya, R.; Thirunavukkarasu, A.; Sathya, A.B.; Sivashankar, R. Magnetic materials and magnetic separation of dyes from aqueous solutions: A review. *Environ. Chem. Lett.* **2021**, *19*, 1275–1294. [CrossRef]
93. Govan, J. Recent Advances in Magnetic Nanoparticles and Nanocomposites for the Remediation of Water Resources. *Magn. Chem.* **2020**, *6*, 49. [CrossRef]
94. Wang, D.; An, Y.; Qiang, J.; Yuan, H. Core-shell amorphous metal oxides/metallic glassy particles for absorbing application of toxic heavy metal and electromagnetic wave. *Scr. Mater.* **2017**, *132*, 30–33. [CrossRef]
95. Mendil, R.; Nasrallah, N. Zn-Fe Layered Double Hydroxides Synthesized by Three (03) Methods of Coprecipitation: Application to the Removal of Cochineal Red Dye from Aqueous Solution. *Fibers Polym.* **2021**, *22*, 3358–3367. [CrossRef]
96. Zhang, J.; Li, R.; Ding, G.; Wang, Y.; Wang, C. Sorptive removal of phenanthrene from water by magnetic carbon nanomaterials. *J. Mol. Liq.* **2019**, *293*, 111540. [CrossRef]
97. Wang, J.; Shao, X.; Liu, J.; Zhang, Q.; Ma, J.; Tian, G. Insight into the effect of structural characteristics of magnetic ZrO_2/Fe_3O_4 nano-composites on phosphate removal in water. *Mater. Chem. Phys.* **2020**, *249*, 123024. [CrossRef]
98. Guan, Y.F.; Marcos-Hernandez, M.; Lu, X.; Cheng, W.; Yu, H.Q.; Elimelech, M.; Villagran, D. Silica Removal Using Magnetic Iron-Aluminum Hybrid Nanomaterials: Measurements, Adsorption Mechanisms, and Implications for Silica Scaling in Reverse Osmosis. *Environ. Sci. Technol.* **2019**, *53*, 13302–13311. [CrossRef]
99. Ananya, R.; Balakrishna, J.; Richard, D. Design of soft magnetic Materials. *arXiv* **2021**, arXiv:2111.05456.
100. Liu, W.K. Preparation of Nano-Adsorption Materials and Study on the Removal Mechanism of Hexavalent Chromium Ion in Water. Master's Thesis, Anhui University of Science and Technology, Huainan, China, 2018. [CrossRef]
101. He, J.Y. Design, Preparation and Removal Mechanism of Hydroxylapatite Nanomaterials. Ph.D. Thesis, University of Science and Technology of China, Hefei, China, 2018.
102. Wen, T. Study on the Removal of Pollutants in Water by Nano-Adsorption Materials and Its Mechanism. Ph.D. Thesis, University of the Chinese Academy of Sciences, Beijing, China, 2016.
103. Plastiras, O.E.; Deliyanni, E.; Samanidou, V. Applications of Graphene-Based Nanomaterials in Environmental Analysis. *Appl. Sci.* **2021**, *11*, 3028. [CrossRef]